01 Apr 1991

Transport Anomalies in the High-Temperature Hopping Conductivity and Thermopower of Sr-doped La(Cr,Mn)O_3

Ryne P. Raffaelle

Harlan U. Anderson
Missouri University of Science and Technology, harlanua@mst.edu

Don M. Sparlin
Missouri University of Science and Technology, sparlin@mst.edu

Paul Ernest Parris
Missouri University of Science and Technology, parris@mst.edu

Recommended Citation

R. P. Raffaelle et al., "Transport Anomalies in the High-Temperature Hopping Conductivity and Thermopower of Sr-doped La(Cr,Mn)O_3," *Physical Review B (Condensed Matter)*, vol. 43, no. 10, pp. 7991-7999, American Physical Society (APS), Apr 1991.
The definitive version is available at https://doi.org/10.1103/PhysRevB.43.7991

Transport anomalies in the high-temperature hopping conductivity and thermopower of Sr-doped La(Cr,Mn)O_3

R. Raffaelle, H. U. Anderson, D. M. Sparlin, and P. E. Parris
Departments of Physics and Ceramic Engineering, University of Missouri–Rolla, Rolla, Missouri 65401
(Received 27 August 1990)

A minimum exists in the electrical conductivity of the perovskite-type ceramic $LaCr_{1-x}Mn_xO_3$ as a function of Mn content near $x=0.05$. This minimum has been explained in terms of a crossover from multiple trapping to percolation among energetically lower Mn sites. In this paper electrical conductivity and Seebeck measurements are presented on a similar series in which 10 mol % Sr was substituted for La in order to increase the small polaron concentration through the compensation of Sr ions according to the Verway mechanism. The data suggests that there is an apparent suppression of the Verway compensation mechanism in all Mn-doped samples. The hopping crossover observed in the Sr-free series is retained with Sr doping, although the position and depth of the electrical-conductivity minimum are altered. Difficulties in the present understanding and interpretation of the electrical conductivity and Seebeck measurements as a function of Mn and Sr content in these materials are discussed. An electronic structure is suggested, which seems to resolve many of these problems.

I. INTRODUCTION

The class of materials known as perovskites or pseudoperovskites has received considerable attention over the past 30 years due to the fact that they often exhibit properties considered useful for the development of thermoelectric devices; e.g., high melting points, a wide range of thermal and electrical conductivities, ferroelectricity, and ferromagnetism.[1] The basic pervoskite structure is represented by the formula ABO_3 in which A, the large cation site, may be an alkali, akaline-earth, or rare-earth ion, and B, represents a transition-metal cation. While the ideal pervoskite structure is cubic, the majority of the ABO_3-based compounds deviate slightly from the cubic structure and form orthorhombic, rhombohedral, or tetragonal "pseudopervoskite" structures.

The search for materials that possess the structural stability and electrical conductivity required in fuel-cell applications has led to the investigation of a number of substitutionally mixed perovskites.[2] Many of these mixed systems involve compounds prepared with two or more isovalent species of B-site ion in an attempt to retain in the composite the desirable properties (e.g., high conductivity, chemical stability) found in the end members. Another class of substitutions is based on the so-called Verway controlled ionic valency principle in which the conductivity of a transition-metal oxide is controlled by substituting donors or acceptors for parent A-site cations in the pervoskite structure in order to effect changes in the carrier concentration found on the B-site cations.[3]

A series which has prompted considerable recent investigation[4–7] due to its potential usefulness in fuel cells is $LaCr_{1-x}Mn_xO_3$. The end member, $LaCrO_3$, exhibits a thermally activated high-temperature electrical conductivity due to p-type small polaron hopping among the B-site cations and is extremely stable to high temperatures over a wide range of oxygen partial pressures. The less-stable $LaMnO_3$ has been thought to conduct via the same mechanism as $LaCrO_3$, but has a significantly greater conductivity. Attempts at substituting Mn for Cr in $LaCrO_3$ to incorporate the increased conductivity found in $LaMnO_3$ have led to some unexpected results.[7] Most notably, the substitutional inclusion of a relatively small amount of Mn has been found to cause the electrical conductivity to drop orders of magnitude below that of either end member. This decrease leads to a minimum in the electrical conductivity at about 5 mol % Mn content. In a recent paper[8] this behavior was attributed to the existence of a significantly lower small-polaron site energy at those B sites in which Mn has been substituted for Cr. According to this interpretation, a small concentration of Mn sites or small clusters can act as traps for carriers diffusing among Cr sites. In this limit ($x \ll 1$) conduction is dominated by multiple trapping, and hence the conductivity is decreased from that of pure $LaCrO_3$. At higher Mn concentrations direct transport among extended percolating clusters of Mn traps becomes possible and the conductivity rises. These two different conduction regimes have traditionally been analyzed in terms of separate (but closely related) models of hopping transport in disordered systems. The multiple-trapping behavior is usually analyzed in terms of a random-well model,[9,10] while dynamical percolation is more typically analyzed using a random-barrier model.[9,11] As discussed below, the La(Cr,Mn)O_3 system is interesting in that it shows that real disordered systems can display aspects associated with both models.

In this paper, a more complete description of the earlier work[8] on the La(Cr,Mn)O_3 series is provided, along with additional electrical conductivity and Seebeck coefficient measurements for a related series containing a small fraction (10 mol %) of Sr substituted for La. The motivation for studying the Sr-doped series was to increase the carrier concentration, and thereby sort out the

carrier density versus mobility dependence of the conductivity previously measured in the undoped series. The multiple-trapping behavior observed at low Mn concentrations was expected to be sensitive to the ratio of charge carriers to traps in the system. Thus, the dependence of the conductivity minimum upon carrier concentration was viewed as a means of testing the crossover interpretation offered in Ref. 8.

As anticipated, crossover behavior is retained in the Sr-doped series. A shift to higher Mn concentration in the position of the conductivity mimimum does occur. In order to obtain a consistent interpretation of both the doped and undoped electrical conductivity and thermopower, it appears necessary to conclude that the Verway mechanism is suppressed in all Mn-doped samples: i.e., the addition of 10 mol % Sr does not seem to result in the expected increase in the number of B-site small polarons, except in the $LaCrO_3$ end member. This suppression is nearly complete in members of the Sr-doped samples which contain more than about 20 mol % Mn. This observation raises the question as to how Sr ions are being compensated in these samples.

The paper proceeds as follows. In Sec. II the experimental details of the measurements are described. In Sec. III the results of the electrical-conductivity and thermopower measurements are presented, first for the $La(Cr,Mn)O_3$ series and then for the Sr-doped samples. The final section contains an analysis of the results along with a discussion regarding possible mechanisms which might allow for the Verway compensation of Sr ions without the comcomitant generation of additional mobile carriers.

II. EXPERIMENTAL PROCEDURE

To ensure adequate data for analyzing the compositional dependence of the electrical conductivity, samples of the series $La_{1-y}Sr_yCr_{1-x}Mn_xO_3$ were prepared containing Mn in 10 mol % increments, with values of the mole fraction of Mn ranging from $x=0$ to $x=1$, and the mole fraction of Sr having either the value $y=0$ or $y=0.1$. Additional samples were made in 5 mol % Mn increments in the region $0<x<0.3$ associated with the electrical-conductivity minimum.

Powders for the series were prepared using a method similar to that first outlined by Pechini,[12] which involves measuring precursor amounts of La carbonate, Cr nitrate, and Mn nitrate and dissolving them in a solution of ethylene glycol, citric acid, nitric acid, and water. This solution is then slowly evaporated to an amorphous solid and calcined at 1173 K to remove the organics. In the preparation of these powders, as is the case with most oxides, care must be taken to control the processing factors necessary to produce "homogeneous" single crystals as revealed by the sharpness of x-ray-diffraction profiles. In the samples produced for this study, x-ray-diffraction analysis does not indicate appreciable amounts of any other phase, implying a nearly complete solid solution of the constituents. The powders were uniaxially pressed into wafers, hydrostatically pressed to 40 000 psi to achieve green densities of approximately 60% of their theoretical density, and then sintered in the appropriate atmosphere and temperature to provide final densities with values in the range 85–95 % of the theoretical density associated with the perfect crystal. The $LaMnO_3$ samples were sintered in air at 1623 K, while the $LaCrO_3$ samples required sintering in an atmosphere of 10^{-11} P_{O_2} at 2023 K. Sintering conditions for samples of mixed composition varied smoothly between these limits. Finally, all samples were annealed in air at 1373 K for 24 h.

Rectangular samples ($1.27\times0.25\times0.25$ cm^3) were cut from the sintered wafers and electrical contacts were made with platinum wire and platinum fire-on paste. The sample edges were notched at four lengthwise increments to aid in the attachment of the platinum wires. Platinum paste was used to cover the ends of the sample in an attempt to provide a uniform current density throughout its length. The resistance as a function of temperature was measured using a four-point-probe technique.

Thermoelectric-power measurements were performed on similar rectangular samples cut from the same wafers as were the conductivity samples. Thermocouples (Pt-Pt/Rh) were kept in electrical and thermal contact with platinum discs, which were attached to the sample ends using platinum paste. A platinum wire heater beyond one of the platinum contact discs was then used to provide a thermal gradient across the sample, while the thermocouples were used to measure the resulting temperature difference. After computer-controlled switching, the platinum legs of the two thermocouples were used to measure the potential difference across the sample. The temperature gradient was varied to obtain a plot of ΔV versus ΔT, the slope of which was determined by a least-squares analysis. This slope, representing the apparent Seebeck coefficient, was then corrected (see Ref. 13) by adding the temperature-dependent absolute thermopower for platinum[14] (which is negative over the temperature range of the measurements), which reduces the apparent Seebeck coefficient. This corrected value was taken to be the Seebeck coefficient of the sample. The apparatus used allowed for three identical probes to be placed in an atmosphere-controlled $MoSi_2$ furnace, thereby allowing for the determination of the Seebeck coefficient as a function of both temperature and oxygen partial pressure.[15]

III. RESULTS

A. The $La(Cr,Mn)O_3$ series

At high temperatures, the mobility of small polarons in a pure single-phase material is proportional to the rate W for hopping between degenerate neighboring polaron sites. This rate takes different forms in different parameter regimes. In the so-called adiabatic limit, the relevant optical-mode lattice fluctuation (of frequency ω_0) is long lived compared to the electron-tunneling event and the hopping rate is given by the expression[16]

$$W=\omega_0\exp(-E_a/kT)\ . \tag{1}$$

In the nonadiabatic limit the electron-tunneling event is not necessarily fast compared to the relevant optical-mode lattice fluctuation. The hopping rate then carries a

temperature-dependent prefactor. In the limit in which the electron-transfer matrix element J is assumed to be much smaller than the lattice relaxation energy E_r, the hopping rate can be expressed in the high-temperature form[16]

$$W=\frac{J^2}{\hbar}\left[\frac{\pi}{4E_akT}\right]^{1/2}\exp(-E_a/kT)\ , \tag{2}$$

in which the small-polaron activation energy E_a is related (but not in general identical) to E_r.

At a finite fractional concentration c of small polarons the hopping rate is reduced due to site blocking, i.e., the possibility that the neighboring site may already be occupied by a charge carrier. In the simplest approximation, which ignores all but the on-site Coulomb repulsion, this has the effect of reducing the mobility

$$\mu=\frac{(1-c)eWa^2}{kT} \tag{3}$$

by a factor of $(1-c)$ from what it would be in the dilute limit.[17] For a low, but temperature independent small-polaron concentration $p=c/\Omega$, where Ω is the unit-cell volume, the conductivity $\sigma=pe\mu$ should be thermally activated with an algebraic prefactor of the form T^{-s} with $s=1$ (adiabatic limit), or $s=\frac{3}{2}$ (nonadiabatic limit). The logarithm of the product σT^s should exhibit a straight line when plotted as a function of the inverse temperature.

It is possible to estimate from the magnitude of the conductivity which form of the prefactor should be used. For example, Emin and Holstein give the inequality

$$\hbar\Omega_0=J^2\left[\frac{\pi}{4E_akT}\right]^{1/2}\ll\hbar\omega_0 \tag{4}$$

as the condition required for the validity of the nonadiabatic limit. In this limit, however, the conductivity is given from Eqs. (2) and (3) by the expression

$$\sigma=\frac{c(1-c)e^2J^2}{\hbar kTa}\left[\frac{\pi}{4E_akT}\right]^{1/2}\exp(-E_a/kT)\ . \tag{5}$$

To be self-consistent, Eqs. (4) and (5) imply that in the adiabatic limit,

$$\Omega_0=\frac{\sigma akT}{c(1-c)e^2}\exp(E_a/kT)\ll\omega_0\ . \tag{6}$$

Taking a from the lattice spacings, the carrier density c from Seebeck coefficient measurements (see Fig. 3), and the activation energy E_a from fits to the measured conductivity (described below), one obtains values of $\Omega_0\cong10^{12}$ Hz for $LaCrO_3$ and $\Omega_0\cong10^{13}$ Hz for $LaMnO_3$. Optical-phonon frequencies for similar materials[18] lie in the range $\omega=10^{13}-10^{14}$ Hz. This suggests that the nonadiabatic limit, Eq. (5), is appropriate for this series, although $LaMnO_3$ lies close to the transition region separating adiabatic from nonadiabatic behavior.

The conductivity of the end members of the La(Cr,Mn)O_3 series does exhibit the activated behavior expected from small-polaron transport over a wide temperature range (see Fig. 1), with $s=\frac{3}{2}$ giving a slightly better fit than $s=1$. A least-squares fit based upon Eq. (5) gives an activation energy of 180±2 meV for $LaCrO_3$ and 190±1 meV for the $LaMnO_3$ data. These values are within 5 meV of the values found in previous studies.[6,7] The differences which do exist between the values reported here and in previous studies may be attributable to the nonadiabatic form which we have assumed in the present study (in contrast to the adiabatic form used to analyze the earlier data), or to different preparation and measuring techniques (i.e., sintering or measuring atmospheres).

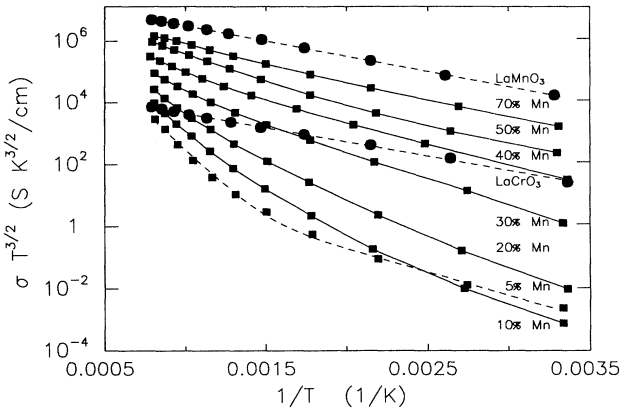

FIG. 1. Logarithmic plot of $\sigma T^{3/2}$ as a function of inverse temperature for the series La(Cr,Mn)O_3. Circles represent end members and squares represent mixed samples. Dashed lines are theoretical fits to the data.

Although the activation energies of the end members are quite similar, $LaMnO_3$ has a conductivity which is approximately 600 times greater than that of $LaCrO_3$. Assuming that Eqs. (2) and (3) apply, this difference could arise from a larger nearest-neighbor electronic coupling factor J in $LaMnO_3$, or from differences in the intrinsic small-polaron concentration c. The low mobility in these materials makes Hall-effect measurements difficult. Thus, information regarding the carrier concentration is often obtained from measurements of the Seebeck coefficient.[13] The Seebeck coefficient represents the transport entropy per charge carrier (experimentally, the thermally induced voltage per degree of temperature difference maintained across the sample in the absence of current flow). Carriers having only one accessible state per site, with multiple occupancy forbidden, have a Seebeck coefficient given by Heikes formula,[13]

$$S=\frac{k}{e}\ln\left[\frac{1-c}{c}\right]+S_0\ , \tag{7}$$

which relates S to the fractional small-polaron concentration c. In Eq. (7), S_0 represents the vibrational entropy per particle and is estimated[13] to be on the order of or less than 10 μV/K. This is often small compared to the carrier-dependent term, and therefore neglected. Note also, that this expression ignores the spin degeneracy of the carriers and implicitly assumes that there is only one allowed spin orientation per site. Neutron-diffraction ex-

periments[19] indicate that $LaMnO_3$ contains antiferromagnetically coupled ferromagnetic planes. It is therefore not unreasonable to expect that the magnetic ordering at each site determines the allowed spin orientation of the small polaron. Equation (7) then provides a temperature-independent relationship between the experimentally measured Seebeck coefficient and the carrier concentration, i.e.,

$$c = \left[1 + \exp\left[\frac{e(S - S_0)}{k}\right]\right]^{-1} . \quad (8)$$

While the end-member Seebeck coefficients are reasonably temperature independent, the Seebeck data for samples containing both Mn and Cr is obviously temperature dependent, especially below 800 K (see Fig. 2). This behavior would appear to make any application of Heikes's formula to the mixed samples problematic. It is not clear at this point what modifications of Heikes's formula would be necessary to account for the temperature dependence observed in the Seebeck voltages of the mixed samples; however, it is generally expected that any model involving carriers distributed over energetically inequivalent sites will reduce to Heikes's formula in the extreme high-temperature limit. Application of Eq. (8) (with $S_0 = 0$) to the highest-temperature Seebeck data from our samples yields the carrier concentrations plotted in Fig. 3. For the end members it is found that $c = 0.01 \pm 0.001$ for $LaCrO_3$, and $c = 0.51 \pm 0.03$ for $LaMnO_3$.

The relative magnitude of the carrier concentrations as inferred from the Seebeck data is, therefore, qualitatively consistent with the large increase in conductivity seen in going from $LaCrO_3$ to $LaMnO_3$. However, the magnitudes of the Seebeck coefficients measured for $LaMnO_3$ are comparable to estimates of the vibrational entropy S_0, which raises questions regarding the appropriateness of neglecting this term. However, a value of S_0 which is of order 10 μV/K would result in a change in the carrier density of $LaMnO_3$ using Eq. (8) of at most 6%. This uncertainty is reflected in the margins of error quoted above for $LaMnO_3$.

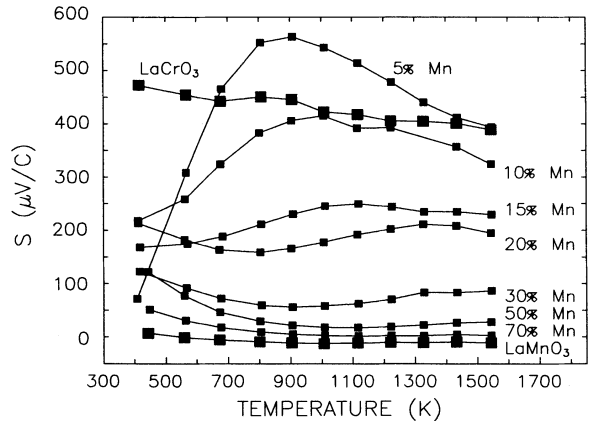

FIG. 2. Seebeck coefficient as a function of temperature for the series $La(Cr,Mn)O_3$. Large squares represent end members and small squares represent mixed samples.

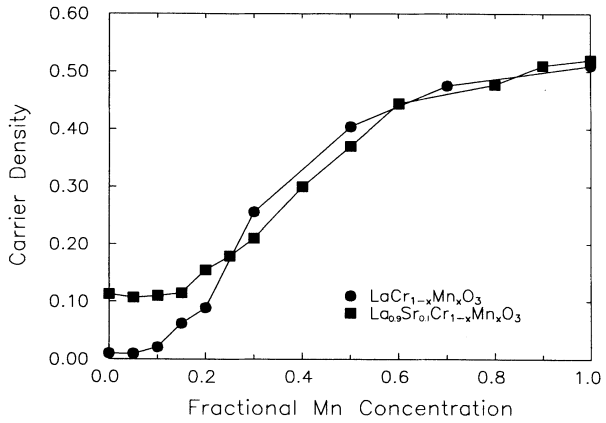

FIG. 3. Carrier density vs Mn content at 1300 K for the series $La(Cr,Mn)O_3$ and $La_{0.9}Sr_{0.1}(Cr,Mn)O_3$, as ascertained by the application of Heikes's formula to the Seebeck coefficient data of Figs. 2 and 7.

The suggested value of $c = 0.01$ for $LaCrO_3$ is not unreasonable if one assumes that the intrinsic carriers in these systems are due to naturally occurring structural defects or impurities. The value $c = 0.51$ obtained for $LaMnO_3$, however, suggests that every other Mn site in this end member is occupied by a Mn^{+4} small polaron. Thermogravimetric analyses show that the amount of excess oxygen in the $LaMnO_3$ when annealed in air is sufficient to account for only a small fraction (~ 0.16) of this apparent carrier concentration.[7] Thus, the large apparent Mn^{+4} concentration seems difficult to reconcile with the average 3+ valence of Mn ions in the structure. We return to this question in Sec. IV.

In spite of the larger intrinsic conductivity of $LaMnO_3$, a small substitution of Mn for Cr in $LaCrO_3$ results in a sharp drop in the conductivity from that exhibited by either of the end members. This minimum, which is more than 4 orders of magnitude below that of $LaCrO_3$ (see Fig. 4), is accompanied by a significant change in the temperature dependence of the conductivity, giving rise to a nonlinear variation of $\ln(\sigma T^{3/2})$ with reciprocal temperature. The maximum curvature (which is positive) is found for a content of 5 mol % Mn, with a slope at the highest temperature corresponding to an activation energy of 1.1 eV.

It is reasonable to associate this high-temperature slope with the activation energy required for a small polaron at a Mn site to make a hop to a neighboring Cr site. This energy would have two primary contributions: one related to the lattice relaxation energy E_r and another from the energy difference $\Delta E = E_{Cr} - E_{Mn}$ between a polaron on a Cr site and one on a Mn site. Assuming the contribution from E_r to be of the same order of magnitude as that of the end members in these and other perovskites,[17] i.e., approximately 100–400 meV, the difference in site energies is estimated to be in the range $\Delta E \sim 700$–1000 meV. Such a relatively large difference in site energy im-

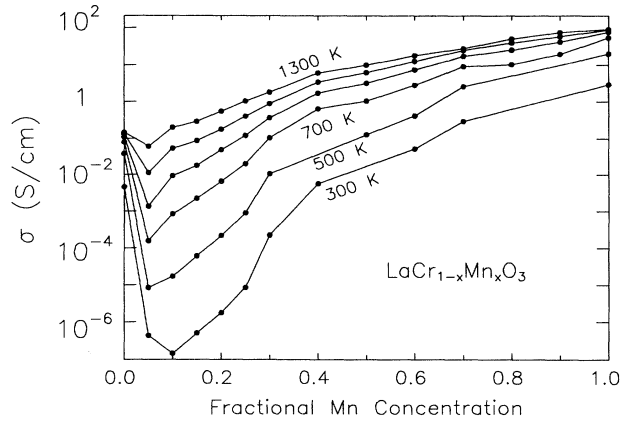

FIG. 4. Conductivity vs Mn content from 300 to 1300 K in 200-K increments for the series La(Cr,Mn)O_3.

plies that a small concentration of energetically lower Mn sites will act as traps for polarons migrating among the Cr ions. A complete description of the conduction process in this system should then involve four nearest-neighbor hopping rates: $W_{c,m}$, $W_{m,c}$, $W_{m,m}$, and $W_{c,c}$, in which $W_{c,m}$ represents the intrinsic hopping rate from a Cr site to a neighboring Mn site, and similarly for the rest. The rate and activation energy for hops between adjacent Cr sites have no particular relation to the rate for hops between Mn sites, although as the end members show, the corresponding activation energies appear to be quite similar in the pure series. Detailed balance considerations stemming from the requirement that the system achieve thermal equilibrium would require that forward and backward hopping rates between sites differing in energy by an amount ΔE be related to one another through a Boltzmann factor, i.e., $W_{m,c}/W_{c,m} \sim \exp(-\Delta E/kT)$. Thus, in the temperature range considered, we would expect the rate for hopping out of a Mn site and onto a neighboring Cr site to be exponentially smaller than either the rate associated with the reverse jump or the rate for jumping between adjacent pairs of similar sites.

Thus, in the small x limit, a single polaron migrating on the predominantly Cr sublattice will at some point make a transition into an isolated energetically lower Mn site. A comparably large amount of time, $\tau \sim 1/W_{m,c}$, must then elapse before the polaron can hop back onto a neighboring Cr site, from which it can continue its migration through the crystal. In the theory of disordered systems this type of transport is referred to as "multiple trapping" or "trap-limited diffusion," and has been shown to lead to a conductivity which can be entirely dominated by the slower rate for leaving the energetically lower state.[9,10]

To quantatively test this trap-limited picture of conduction for the 5 mol % Mn samples, a modification was made to include the effects of site blocking by other carriers in a two-state version of the random-well model considered in several earlier theoretical studies.[9,10] The modification involves the consideration of charge carriers in fractional concentration c distributed in equilibrium over a lattice containing sites associated with one of two different energies. Let x_1 and $x_2=1-x_1$ denote the fraction of sites associated with energies E_1 and E_2, respectively, with $E_2 \ll E_1$ and $x_2 \ll x_1$. Thus, the lower-energy states nearly always occur as isolated traps for carriers migrating among the higher-energy states, and the rate for hopping out of the traps is presumed to be exponentially lower by a Boltzmann factor than the rate for hopping out of the higher-energy states. Assuming that no two carriers can occupy the same site, then the mole fraction of carriers in sites of energy E_i at temperature $T=1/k\beta$ will be given by the two-state Fermi-gas expression $c_i=x_i[z^{-1}\exp(\beta E_i)+1]$, where the fugacity $z=\exp(\beta\mu)$ is easily determined from the quadratic equation that follows from setting $c_1+c_2=c$. Thus, a "tagged" carrier migrating in this random-trapping environment sees a lattice which contains the following: a molar concentration $q=(x_2-c_2)$ of "unfilled" deep wells into which it can get trapped for a long time before getting out; a fraction $c=(c_1+c_2)$ of inaccessible (occupied) sites of both types, and a fraction $(x_1=c_1)$ of accessible shallow wells. In the limit that $c \ll x_1$, the fraction of blocked shallow wells is small and can, within the same approximation implicit in Eq. (3), be taken into account by simply reducing the hopping rate for hops into the shallow wells by the probability of their being blocked. Thus, let W_{ij} denote the hopping rate from states of energy E_i to states of energy E_j for a single particle in the absence of site blocking. In the presence of a finite concentration of carriers the hopping rate for a tagged particle will be $w_2=(1-c)W_{21}$ when hopping out of the deep wells (of energy E_2) and $w_1=(1-c)W_{11}$ when hopping out of the shallow wells (of energy E_1). The exact result for the diffusion constant of a particle in a disordered environment containing a distribution of wells of random depth is then given through the analyses of Refs. 9 and 10 by the expression $D=W_{\rm eff}a^2$, with $W_{\rm eff}=\langle 1/W\rangle^{-1}$, in which the average is over all possible configurations of the disordered environment. In the present circumstance this leads to the expression

$$W_{\rm eff}=\left[\frac{q}{(1-c)W_{21}}+\frac{1-q}{(1-c)W_{11}}\right]^{-1}. \tag{9}$$

The lower dashed curve in Fig. 1 is obtained using this expression taking $x_2=x=0.05$, $c=0.0505$, and $\Delta E=0.7$ eV. The hopping rate W_{12} out of the higher-energy Cr sites has been taken from the fit to the end member $LaCrO_3$ data, while the hopping rate W_{21} out of the lower-energy Mn sites has been derived using the 1.1-eV activation energy associated with the high-temperature Arrhenius slope seen in the 5 mol % Mn sample. Interestingly, we find that in order to obtain the positive curvature exhibited by the 5 mol % Mn data, it is necessary to have a carrier-to-trap density ratio which is slightly greater than unity, implying that the carrier concentration increases linearly with the concentration of traps. Nonetheless, the quantative agreement with the 5 mol % Mn data does appear to be consistent with the interpretation of the conduction mechanism in this regime as being due to multiple trapping.

As the Mn concentration is increased past some critical concentration, a connected path of Mn sites spanning the crystal will inevitably form. Once this occurs, particles trapped in an extended cluster of Mn traps will no longer need to make a transition onto a Cr site in order to participate in conduction. Hence, the conductivity will no longer be limited by the slow rate $W_{m,c}$, and the trap-limited picture will no longer apply. Instead, conduction should cross over to a percolative regime[11] characterized by a conductivity which increases with Mn concentration above the critical concentration and an activation energy which approaches that associated with the rate $W_{m,m}$ of the end-member $LaMnO_3$. For isotropic site percolation in a cubic lattice,[11] under the assumption that the substituted Mn ions randomly occupy Cr sites in the cubic B-site sublattice, an increase in conductivity should occur in the vicinity of the critical concentration $x_c \sim 0.31$.

The conductivity data does exhibits percolationlike behavior, as shown by the Arrhenius plots of $\ln(\sigma T^{3/2})$ versus $1/T$ in Fig. 1. A large increase in conductivity occurs in the neighborhood of $x \sim 0.30$, and the temperature dependence for samples with $x > 0.30$ is characterized by an activation energy (slope) which becomes progressively closer to that of the end member as x increases. The small increase in slope at higher temperatures may be due to the ability of carriers to occasionally pass through the energetically higher Cr sites, rather than having to go around them as would be required if the carriers were strictly confined to Mn sites. To facilitate comparison to the percolation model, a linear plot of normalized conductivity σ/σ_{Mn} as a function of Mn composition at 1273 K is presented in Fig. 5, along with simulation data for the site-percolation model taken from Kirkpatrick.[11] {The experimental data of Fig. 5 have also been corrected for density and carrier concentration by multiplying by $\rho(1)/\rho(x)$ and $c(1)[1-c(1)]/c(x)[1-c(x)]$, where $\rho(x)$ is the measured density with Mn mole fraction x and $c(x)$ is taken from Fig. 3.} For Mn concentrations above the critical concentration, the measured conductivities approach the site-percolation curve from below with increasing temperature. This drop below the percolation curve at lower temperatures could arise from the presence of a (relatively narrow) distribution of energetically inequivalent sites within the Mn sublattice itself, the effects of which become less important at higher temperatures. The site-percolation curve goes to zero at the critical point. Thus, it is not unexpected that the experimental conductivity, in the process of crossing over to the multiple-trapping regime, becomes greater than the percolation curve in the neighborhood of the critical concentration. In the crossover region, $0.1 < x < 0.3$, there is a general increase in conductivity with increasing x. This may simply reflect a small-polaron concentration that is increasing with Mn content in this region (see Fig. 3), in which case a strictly nearest-neighbor model may suffice for analyzing the crossover. Alternatively, if any of the greater than nearest-neighbor Mn-to-Mn hopping rates are significantly larger than the nearest-neighbor Mn-to-Cr rate, the increase could be an effect associated with the diminishing separation distance between isolated Mn sites and, possibly, a percolation transition of greater than nearest Mn neighbors.[20] Neither of these alternatives should affect the interpretation of the large $x > 0.3$ and small $x \sim 0.05$ regimes.

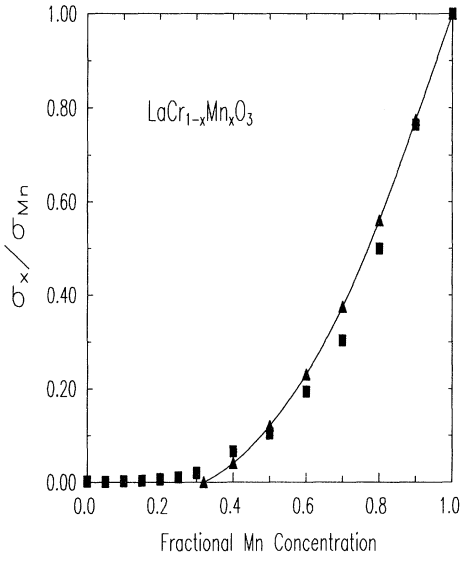

FIG. 5. Normalized conductivity vs Mn content for the series $La(Cr,Mn)O_3$. Triangles represent site-percolation data from Ref. 11.

B. The series (La,Sr)(Cr,Mn)O_3

As Fig. 6 shows, the Arrhenius plots for the end members of the Sr-doped series also exhibit a linear behavior over a wide temperature range, although the activation energies have changed as a result of Sr doping. The end-member activation energies of the Sr-doped series have values of 141±2 meV for $La_{0.9}Sr_{0.1}CrO_3$ and 206±2 meV for $La_{0.9}Sr_{0.1}MnO_3$. This is a decrease with Sr-doping of nearly 40 meV from the activation energy of $LaCrO_3$ and an apparent increase of approximately 20

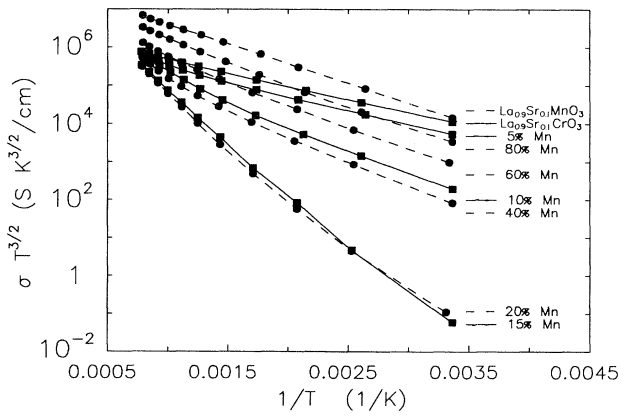

FIG. 6. Logarithmic plot of $\sigma T^{3/2}$ as a function of inverse temperature for the series $La_{0.9}Sr_{0.1}(Cr,Mn)O_3$.

meV over that of $LaMnO_3$. The decrease in activation energy for the Cr samples is comparable to that which has been found in previous studies.[6] The 20-meV increase in activation energy observed in the $(La,Sr)MnO_3$ series when measured in air is in the opposite direction to the change observed in other studies[7] on Sr-doped $LaMnO_3$, which have shown a decrease in activation energy upon Sr addition when measured in oxygen. The microscopic basis for these differences in activation energy when measured under different oxidizing conditions is currently under investigation.

It is interesting to note that the conductivity of $LaCrO_3$ increases with Sr doping as expected from Verway's principle, while the conductivity increase in $LaMnO_3$ is considerably less than expected. The largest fractional increase in conductivity in the Cr samples occurs at room temperature, with the 10 mol % Sr addition giving rise to an increase in conductivity by a factor of 400. This large increase in the room-temperature conductivity, along with application of Heikes's formula to the high temperature Seebeck data (Figs. 2 and 7), suggests an increase in the molar carrier density from approximately $c=0.01$ to 0.10 with the addition of 10 mol % Sr (see Fig. 3). This increase is essentially equivalent to the amount of Sr added, consistent with Verway's principle which would suggest that Sr is compensated in $LaCrO_3$ by the transition of Cr^{3+} ions into mobile Cr^{4+} polarons as expected.

This does not appear to be the case for $LaMnO_3$, however. The maximum observed increase in the conductivity of the end-member Mn samples with 10 mol % Sr addition occurs at high temperatures and is less than a factor of 2. The minimal change observed in both the conductivity and in the high-temperature Seebeck coefficient when 10 mol % Sr is added to $LaMnO_3$ suggests that there is in fact very little change in the carrier density (see also Fig. 3). If this interpretation is correct, it suggests that Verway's principle is not obeyed for this system, and raises the obvious question as to how Sr is electronically compensated in the $La_{0.9}Sr_{0.1}MnO_3$ structure.

As Fig. 8 shows, the multiple-trapping and/or percolation crossover identified in the $LaCr_{1-x}Mn_xO_3$ series is qualitatively unchanged with the addition of 10 mol % Sr. Indeed, the agreement of the normalized conductivities in the pure and Sr-doped series above the transition region is striking (see Fig. 9). The relative position and depth of the minimum in the electrical conductivity as a function of Mn concentration is altered with Sr doping. When 10 mol % Sr is added to the $LaCr_{1-x}Mn_xO_3$ series, there is a shift in the conductivity minimum from approximately 5 mol % Mn to 15 mol % Mn (see Figs. 4 and 8). Indeed, it appears that in the Sr-doped, 5 mol % Mn sample there is a substantial excess of carriers to traps, so that any given carrier sees very few unblocked traps in its path. As a result, the conductivity of this sample resembles that of the end member ($x=0$), although it is reduced somewhat in magnitude by residual trapping effects. By contrast, the relative depth of the

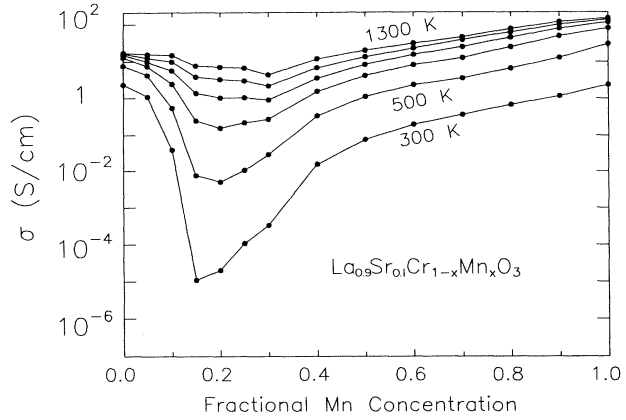

FIG. 8. Conductivity vs Mn content for $La_{0.9}Sr_{0.1}(Cr,Mn)O_3$ for 300–1300 K in increments of 200 K.

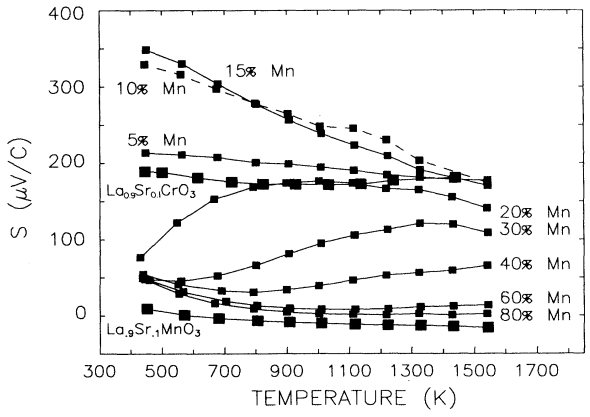

FIG. 7. Seebeck coefficient vs temperature for the $La_{0.9}Sr_{0.1}(Cr,Mn)O_3$ series. Large squares represent end members and small squares represent mixed samples.

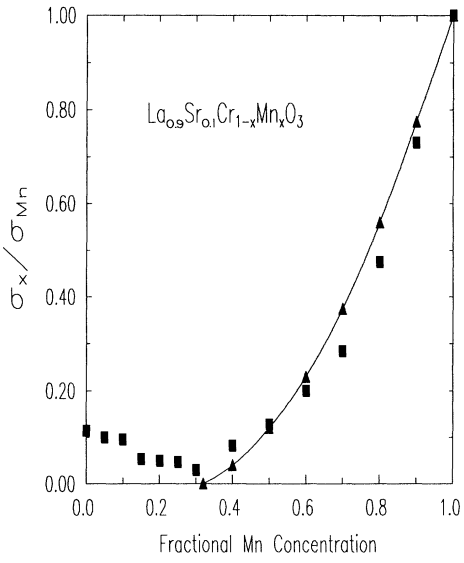

FIG. 9. Normalized conductivity vs Mn content of the series $La_{0.9}Sr_{0.1}(Cr,Mn)O_3$. Triangles represent site-percolation data from Ref. 11.

conductivity minimum with respect to the $LaCrO_3$ end member has increased from approximately 4 orders of magnitude in the undoped sample, to approximately 5 orders of magnitude with the addition of Sr.

Perhaps the most surprising feature in the Sr-doped samples, however, is the absence of a significant change in either the electrical conductivity or in the high-temperature Seebeck coefficient with Sr addition for samples containing more than 30 mol % Mn. Also, note from Fig. 3 the smooth increase in carrier concentration with small Mn substitution ($x < 20\%$) which occurs in the non-Sr-doped series (as determined by the high-temperature Seebeck data). A similar increase in carrier concentration does not appear to occur in the Sr-doped samples, which show nearly constant carrier densities in this region. As in the $LaMnO_3$ end member, this appears to suggest a Sr compensation mechanism which does not involve the creation of mobile *B*-site small polarons.

IV. DISCUSSION

The electrical conductivity of the $(La,Sr)(Cr,Mn)O_3$ series demonstrates behavior which is consistent with the previously identified crossover in electrical conduction from multiple trapping to percolation. This crossover, which persists with the addition of Sr, is qualitatively explainable in terms of a relatively simple two-state model based upon the assumption that Mn sites lie lower in energy than Cr sites. Clearly, however, the quantitative behavior seen in the Sr-doped samples has raised a number of new questions regarding the nature of electrical conduction in these materials. Specific questions which emerge from the present study include the following:

(i) Why do Seebeck and electrical-conductivity measurements indicate little or no increase in the carrier density in $LaMnO_3$ with Sr doping, as would be expected from Verway's principle (particularly since the Verway mechanism appears to hold for $LaCrO_3$)?

(ii) What is the source of the apparently large intrinsic carrier concentration ($c = 0.51 \pm 0.03$) in $LaMnO_{3+\delta}$? As we have observed, this value does not agree with previous estimates[7] of the oxygen over-stoichiometry ($\delta \sim 0.08$). Indeed, in one study, Kuo *et al.* observed no apparent change in either the conductivity or Seebeck coefficient under mildly reducing conditions in which excess oxygen was removed and stoichiometry achieved.

(iii) Why is the carrier concentration (as determined by Heikes's formula) roughly constant in the 10 mol % Sr-doped samples below 20 mol % Mn, and why is there so little change from the pure series observed above 30 mol % Mn when 10 mol % Sr is added?

(iv) What accounts for the apparent increase in carrier concentration with increasing Mn (specifically, a carrier-to-trap ratio exceeding unity) in the trap-limited region, as is revealed in the fits of the conductivity data to the two-state random-well model for $x = 0.05$.

Any explanation of these questions must obviously reconcile the apparently large Mn^{4+} concentration with the average 3+ valence of the Mn ions in the $LaMnO_3$ structure. One clue to a possible electronic structure which might explain these observations can be found in the pseudoperovskite $BaBiO_3$. It has been reported that the average 4+ valence of the Bi ions is disproportionated into stabilized Bi^{3+}-Bi^{5+} pairs.[21] If a similar stabilization of Mn^{3+} ions into Mn^{2+}-Mn^{4+} pairs were to occur in $LaMnO_3$ it would offer an explanation of the apparent carrier density of approximately 0.5 deduced for this material from analysis of the Seebeck coefficient data. If, in addition, we assume that Sr introduced into $LaMnO_3$ is preferentially compensated through the conversion of Mn^{2+} into Mn^{3+}, it would explain the apparent lack of change in the Mn^{4+} small-polaron density with Sr addition for samples containing Mn concentrations greater than 30 mol % Mn.

An explanation of the carrier density observed at low Mn concentrations in terms of this pairing model requires some additional assumptions. In particular, if one is to explain the apparent fact deduced from the random-trapping analyses (and qualitatively supported by the Seebeck data) that in the non-Sr-doped samples the carrier concentration increases in direct proportion to the number of Mn traps added to the system, it seems necessary to assume that Mn is preferentially incorporated into the $LaCrO_3$ structure in the form of stabilized Mn^{2+}-Mn^{4+} pairs. Thus every pair which comes into the structure acts as a single trap, but it brings with it one Mn^{4+} small polaron to add to the carrier concentration. This idea is further strengthened when it is observed that if, as in the pure Mn samples, the addition of Sr serves to convert the existing Mn^{2+} into Mn^{3+}, then the resulting carrier dependence on Mn concentration for the Sr-doped sample would appear precisely as it does in Fig. 3. At 0 mol % Mn all the Sr is compensated by the conversion of Cr^{3+} into Cr^{4+}. At 5 mol % Mn, approximately 2.5 mol % (the approximate concentration of Mn^{2+}) of the 10 mol % Sr addition is compensated by the conversion of Mn^{2+} into Mn^{3+}. Since Mn^{5+} cannot be produced, the remaining 7.5% Sr is all compensated by the conversion of Cr^{3+} into Cr^{4+}carriers. The net result is a final carrier density of 10 mol %, the same as in the end member. By similar arguments one can see that this mechanism predicts a carrier density that remains unchanged at about 10 mol % in the Sr-doped series until the number of carriers created by the increasing numbers of Mn^{2+}-Mn^{4+} pairs exceeds the 10 mol % associated with the Sr addition. Since one carrier accompanies each Mn^{2+}-Mn^{4+} pair, this should occur at approximately 20 mol % concentration, as seen in Fig. 3.

V. CONCLUSION

Electrical conduction in the $(La,Sr)(Cr,Mn)O_3$ system exhibits a crossover between two different mechanisms, from multiple trapping at low Mn concentrations to percolation of small polarons among the lower-energy Mn sites at higher concentrations. The addition of 10% Sr appears to create a corresponding density of small polarons in pure $LaCrO_3$, but not in pure $LaMnO_3$, or in mixed compounds containing greater than 20 mol % Mn. A picture involving the disproportionation of Mn^{3+} ions into Mn^{2+}-Mn^{4+} pairs seems to provide a compensation mechanism which is able to account for this apparent

buffering of added Sr ions, and also provides a natural explanation for the apparently large number of intrinsic carriers seen in $LaMnO_3$. This work underscores the need for a comprehensive theoretical description of several aspects of the conduction processes occurring in these materials. Specifically, it is hoped that the present study will stimulate the development of a multistate hopping model capable of describing the observed crossover in electrical conductivity, as well as an extension of previously derived theories for the Seebeck coefficient associated with hopping transport in energetically disordered systems. In addition, more experimental and theoretical work is required to either confirm or to elucidate the nature of the electronic and electron-phonon interactions which might lead to the kind of pairing mechanism which has been suggested in this study.

ACKNOWLEDGMENTS

This research was supported by the Basic Energy Science Division, U.S. Department of Energy, under Contract No. DE-FG0285ER45219.

[1]J. B. Goodenough, Prog. Solid State Chem. **5**, 145 (1971).
[2]H. U. Anderson, in *Proceedings of the First International Symposium on Solid Oxide Fuel Cells,* edited by Subash C. Singhal (Electrochemical Society, Pennington, NJ, 1989).
[3]E. J. Verway, P. W. Haaijam, F. C. Romeijh, and G. W. Van Oosterhout, Philips Res. Rep. **5**, 173 (1950).
[4]S. Ranier, German Patent No. 2824408, May 1982.
[5]D. P. Karim and A. T. Aldred, Phys. Rev. B **20**, 2255 (1979).
[6]W. J. Weber, C. W. Griffen, and J. L. Bates, J. Am. Ceram. Soc. **70**, 265 (1987).
[7]J. H. Kuo, H. U. Anderson, and D. M. Sparlin, J. Solid State Chem. **83**, 52 (1989); **87**, 55 (1990).
[8]R. Raffaelle, H. U. Anderson, D. M. Sparlin, and P. E. Parris, Phys. Rev. Lett. **65**, 1383 (1990).
[9]S. Alexander, J. Bernasconi, W. R. Schneider, and R. Orbach, Rev. Mod. Phys. **53**, 175 (1981); J. W. Haus and K. Kehr, Phys. Rep. **150**, 265 (1987).
[10]J. W. Haus, K. Kehr, and J. W. Lylema, Phys. Rev. B **25**, 2905 (1982); K. Kundu and P. Phillips, Phys. Rev. A **35**, 857 (1987).
[11]S. Kirkpatrick, Rev. Mod. Phys. **45**, 574 (1973).
[12]M. Pechini, U.S. Patent No. 3,330,697, July 1967.
[13]R. R. Heikes, *Thermoelectricity* (Wiley-Interscience, New York, 1961).
[14]F. J. Blatt, P. A. Schroeder, C. L. Foiles, and D. Greig, *Thermoelectric Power of Metals* (Plenum, New York, 1976).
[15]G. Carini, M. S. thesis, Univ. of Missouri-Rolla, 1988.
[16]D. Emin and T. Holstein, Ann. Phys. (N. Y.) **53**, 439 (1969); T. Holstein, *ibid.* **8**, 325 (1959); D. Emin, Adv. Phys. **24**, 305 (1975).
[17]J. B. Goodenough, Phys. Rev. **164**, 785 (1967).
[18]J. C. Philips *Physics of High-Tc Superconductors* (Academic, San Diego, 1989).
[19]E. O. Wollan and W. C. Koehler, Phys. Rev. **100**, 545 (1955).
[20]H. Scher and C. H. Wu, Proc. Natl. Acad. Sci. U.S.A. **78**, 22 (1980); J. Chem. Phys. **74**, 5366 (1981); V. Ambegaokar, B. I. Halperin, and J. S. Langer, Phys. Rev. B **4**, 2612 (1971); P. E. Parris, *ibid.* **39**, 9343 (1989).
[21]A. W. Sleight, J. L. Gillison, and P. E. Bierstedt, Solid State Commun. **17**, 27 (1975); D. E. Cox and A. W. Sleight, *ibid.* **19**, 969 (1976); C. Chaillout, A. Santoro, J. P. Remeika, J. S. Cooper, and G. P. Espinosa, *ibid.* **65**, 1363 (1988).